

Materials Science and Engineering A 452-453 (2007) 633-639



Elastic constants and internal friction of martensitic steel, ferritic-pearlitic steel, and α -iron

Sudook A. Kim*, Ward L. Johnson

National Institute of Standards and Technology, Materials Reliability Division, 325 Broadway, Boulder, CO 80305, USA Received 4 August 2006; received in revised form 23 October 2006; accepted 29 November 2006

Abstract

The elastic constants and internal friction of induction hardened and unhardened SAE 1050 plain-carbon steel at ambient temperatures were determined by resonant ultrasonic spectroscopy. The hardened specimen contained only martensite and the unhardened specimen was ferrite-pearlite. Using an inverse Ritz algorithm with assumed orthorhombic symmetry, all nine independent elastic-stiffness coefficients were determined, and, from the resonance peak widths, all nine components of the internal-friction tensor were determined. Similar measurements and analysis on monocrystalline α -iron were performed. The steel has slight elastic anisotropy, and the isotropically approximated elastic moduli were lower in the martensite than in ferrite-pearlite: shear modulus by 3.6%, bulk modulus by 1.2%, Young modulus by 3.2%, and Poisson ratio by 1.5%. Isotropically approximated elastic moduli of α -iron were 0.6–1.3% higher than ferrite-pearlite. All components of the internal-friction in martensite were higher than those of ferrite-pearlite, but lower than those of α -iron. © 2006 Elsevier B.V. All rights reserved.

Keywords: α-Iron; Bulk modulus; Carbon steel; Damping; Elastic constants; Ferrite; Hardness; Induction hardening; Internal friction; Martensite; Iron; Pearlite; Plain steel; Poisson ratio; Resonant ultrasound spectroscopy; Shear modulus; Young modulus

1. Introduction

The elastic moduli of martensitic and ferritic-pearlitic plain carbon steel play a central role in determining the other mechanical properties of induction-hardened parts, including crack resistance arising from compressive residual stress at hardened surfaces. Nevertheless, published experimental measurements of moduli rarely have included both martensitic and ferritic-pearlitic states of a single alloy. Variations in reported values for alloys with similar composition also are significant. In this report, we present resonant ultrasonic measurements of the complete elastic-constant and internal-friction tensors of martensitic and a ferritic-pearlitic plain carbon steel, SAE 1050, which has a medium carbon content of $\sim\!\!0.5\,\mathrm{wt}.\%$. To interpret the results, we also present measurements on monocrystalline bodycentered-cubic iron.

2. Specimens

We extracted two steel specimens from commercially fabricated automotive drive shafts that were induction heated, water quenched to intermediate temperatures, and, then, slowly cooled to ambient temperatures. The material was hot-rolled SAE 1050 steel with composition, in weight percent, of 0.48-0.55 C, 0.9-1.1 Mn, 0.15-0.30 Si, 0.3 Al, <0.05 S, <0.04 P, <0.10 Ni, <0.12 Cr, <0.05 Mo, and <0.18 Cu. The shafts had several grooves and splines machined in the surface, as described elsewhere [1], but the regions from which specimens were taken had a uniform diameter of 23.8 mm. Fig. 1 shows the hardness through surface depths of the two shafts, which are labeled B564 and C322. The Rockwell-C hardness ($R_{\rm C}$) values were derived from microficial hardness data that were provided by the manufacturer.

Specimen B564 showed 58 $R_{\rm C}$ hardness extending to a depth of 3.2 mm from the surface. From this fully hardened region, a rectangular-parallelepiped specimen was made. The dimensions of this specimen were 3.1 mm \times 2.8 mm \times 2.9 mm, corresponding to the radial, azimuthal, and axial directions, respectively, of the cylinder. A second specimen, taken from

^{*} Corresponding author. Tel.: +1 303 497 3424; fax: +1 303 497 5030. E-mail address: sak430@boulder.nist.gov (S.A. Kim).

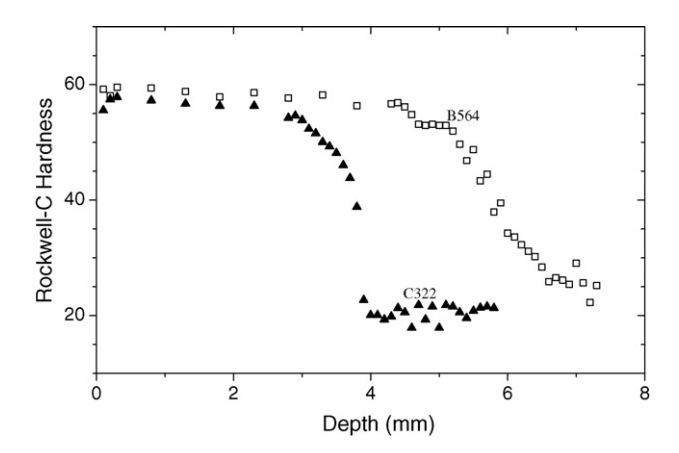


Fig. 1. Hardness vs. depth in induction-hardened shafts. Specimens were taken from regions of nearly constant hardness.

the unhardened center of the shaft C322, had dimensions of $10.7\,\mathrm{mm} \times 9.32\,\mathrm{mm} \times 12.1\,\mathrm{mm}$ and an average hardness of $20\,R_\mathrm{C}$. A third specimen was α -Fe with dimensions of $4.3\,\mathrm{mm} \times 5.2\,\mathrm{mm} \times 4.6\,\mathrm{mm}$ and crystallographic directions [100], [010], and [001] aligned perpendicular to the rectangular faces. Opposite surfaces of the specimens were parallel within $8\,\mu\mathrm{m}$.

We determined mass densities by Archimedes' method using distilled water as a standard. The densities of martensite, ferrite-pearlite, and α -iron were 7.709 ± 0.002 g/cm³, 7.835 ± 0.001 g/cm³, and 7.851 ± 0.011 g/cm³, respectively.

3. Methods

To study elastic stiffness and internal friction of these materials, we used resonant ultrasonic spectroscopy, which has been described in detail elsewhere [2]. Briefly, a piezoelectric transducer produces a sinusoidal vibration at one point on a specimen, and another piezoelectric transducer detects the response of the specimen at a different point. One implementation employs a tripod arrangement, as shown in Fig. 2(a), with the third element acting only to support the specimen. This arrangement was used on the ferrite-pearlite specimen (C322), which had a mass that was large enough to produce sufficient acoustic coupling between the specimen and transducers. For the two smaller specimens, the arrangement shown in Fig. 2(b) was used. The transducers held the specimen by diagonal corners with spring forces that are set low to minimize damping from the mechanical contact. Resonant ultrasonic spectroscopy typically introduces only slight perturbations to the resonance by mechanical contact. In contrast, the more commonly employed method of pulse-echo superposition requires measurements using bonded transducers with more than one orientation and/or polarization, and more than one specimen often is needed to obtain the complete set of elastic constants.

We determined elastic stiffness coefficients C_{ij} using an inverse Ritz analysis [2–4], which requires measured resonant frequencies, specimen shape, mass density, dimensions, and initial realistic guesses for the C_{ij} . The elastic symmetries of the specimens were assumed to be orthorhombic for both hardened

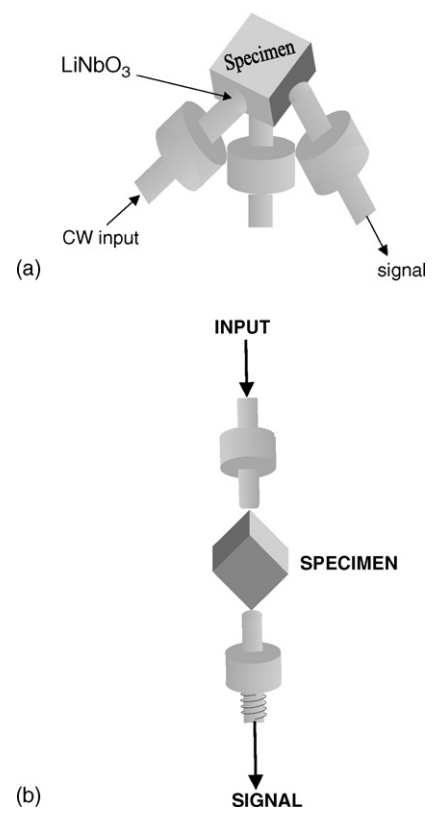


Fig. 2. (a) Tripod specimen holder. One transducer sends a continuous sinusoidal signal with varying frequency, one transducer detects macroscopic resonant frequencies, and the third transducer supports the specimen. Semispherical buffer rods provide a point contact with the specimen. (b) Spring-loaded specimen holder. The fixture holds the specimen at opposite corners to minimize the contact loss.

and unhardened specimens. For each resonance frequency f_n , an internal friction q_n^{-1} also was determined from the full width of the peak δf at $1/\sqrt{2}$ of maximum: $q_n^{-1} = \delta f/f_n$.

The elastic stiffness and internal friction can be considered to be the real and imaginary parts of a complex elastic stiffness tensor \tilde{C}_{ij} : $\tilde{C}_{ij} = C_{ij}(1+iQ_{ij}^{-1})$. The q_n for a given resonance is a function of several components of the internal friction tensor Q_{ij}^{-1} . Following successful convergence of the inverse Ritz analysis, the Q_{ij}^{-1} were determined by solving a set of simultaneous equations.

$$Q_{ij\,\text{calc.}}^{-1} = (J_{nij}^t J_{nij})^{-1} J_{nij}^t q_n^{-1}, \tag{1}$$

where $J_{nij} = 2(C_{ij}/f_n)(\partial f_n/\partial C_{ij})$, J_{nij}^t is the transpose of J_{nij} , and $\partial f_n/\partial C_{ij}$ denotes the variation of resonance frequency with respect to the elastic stiffness. Q_{ij}^{-1} is assumed to have no significant dependence on frequency over the measured range. The validity of this assumption is considered below.

In order to compare the elastic stiffnesses of orthorhombic (nine \tilde{C}_{ij}) martensitic and ferrite-pearlite steels with those of α -Fe (three \tilde{C}_{ij}), all \tilde{C}_{ij} were converted into sets of isotropic elastic moduli (two \tilde{C}_{ij}). The orthorhombic elastic coefficients were converted to shear modulus \tilde{G} and bulk modulus \tilde{B} using the Voigt-Reuss-Hill model [5]. For the cubic elastic stiffness coefficients, the corresponding isotropic shear modulus was cal-

Download English Version:

https://daneshyari.com/en/article/1584148

Download Persian Version:

https://daneshyari.com/article/1584148

Daneshyari.com